DOI:10.2478/auoc-2025-0020

Ovidius University Annals of Chemistry Volume 36, Issue 2, pp. 170 - 185, 2025

Computational investigations of D-glucofuranose-based derivatives: DFT, MEP, NBO, ADMET, PASS, and molecular docking toward antidiabetic targets

Ivy ISLAM and Sarkar M.A. KAWSAR*

Lab of Carbohydrate and Nucleoside Chemistry (LCNC), Department of Chemistry, Faculty of Science, University of Chittagong, Chittagong-4331, Bangladesh

Abstract. A chronic metabolic disease characterized by persistently elevated blood sugar levels, diabetes mellitus is typically caused by inadequate insulin synthesis or function. Because natural monosaccharides and carbohydrates such as D-glucofuranose share structural similarities, they present a promising foundation for the development of antidiabetic drugs. 3-*O*-Acyl derivatives were produced by the unimolar one-step acylation of D-glucopyranose. Computational methods were used to investigate the potential antidiabetic effects of D-glucofuranose (**1**) and its derivatives (**2-9**). The frontier molecular orbital (FMO) characterizes reactivity by analyzing the energy difference between the HOMO (highest occupied molecular orbital) and LUMO (lowest unoccupied molecular orbital) orbitals, whereas the electrostatic potential map (MEP) shows the charge distribution of a molecule, highlighting regions prone to electrophilic and nucleophilic interactions, and global reactivity indicators such as hardness, softness, and electrophilicity characterize a molecule's overall reactivity, which is the outcome of density functional theory (DFT) calculations to optimize the molecule's stable geometric configuration. To estimate the binding affinities and interaction patterns, molecular docking experiments were conducted with human glucokinase (PDB IDs: 3IMX and 1V4S). Compound **7** exhibited the highest binding affinities (-9.0 and -8.2 kcal/mol) and formed persistent interactions with the TRP99, HIS218, VAL62 and IEL211 residues in the glucokinase active site. ADMET estimates were used to evaluate drug similarity, pharmacokinetics and toxicity profiles. *In silico* tests *via* PASS prediction against bacteria and fungi revealed that the compounds containing D-glucofuranose derivatives had outstanding antibacterial and antifungal effectiveness. Overall, these results show that D-glucofuranose derivatives have the potential to be lead molecules for glucokinase regulation and offer a logical framework for further validation *in vitro* and *in vivo*.

***Keywords*:** D-glucofuranose; FMO; MEP; pharmacokinetics; human glucokinase; molecular docking; ADMET.

1. Introduction

Carbohydrates are a class of chemically defined compounds that have various physical and physiological properties as well as health advantages [1]. They are composed of carbon, hydrogen and oxygen generally following a 1:2:1 ratio among the most essential biomolecules in nature. They are the most stereo chemically diverse macromolecules. This intricacy results in highly specialized and selective interactions that can play important roles in protein folding [2]. They are glycans derived from glycoproteins, glycolipids and proteoglycans that bind to proteins or other carbohydrates, facilitating cell-cell and cell-matrix interactions [3]. Carbohydrate metabolism begins with meal digestion in the gastrointestinal system and continues with enterocytes absorbing the carbohydrate components as monosaccharides [4]. They fall into three main categories: polysaccharides, disaccharides and monosaccharides. Glycans (monosaccharide unit linked through glycosidic bond), a distinct class of carbohydrates, are implicated in a wide range of disorders, including cancer, inflammation, and microbial infections. Specific glycan–lectin interactions have been exploited for the development of vaccines, antiviral agents, and immunotherapies [5]. Recently, advanced and sophisticated techniques have facilitated the isolation of diverse natural products from plants [6] and other natural sources, with carbohydrates serving as key constituents [7].

Many physiological processes, such as energy production, metabolism, and the preservation of healthy cellular function, depend on carbohydrates. The body prefers to use carbohydrates as an energy source, especially for muscles, red blood cells, and the brain, when exercising. Upon consumption, glucose is produced by the breakdown of carbohydrates and is subsequently taken up by the bloodstream. The glucose can either be used right away for energy or stored in the muscles and liver as glycogen for later use. Four calories are produced from 1 g of carbohydrates. The body quickly uses glycogen stores to drive muscular contraction and movement during periods of high physical activity [8]. Since glucose serves as the brain's primary fuel, carbohydrates play a critical role in the metabolic synthesis of energy. Glucose reliance stems from the high metabolic demands of brain processes such as synaptic transmission, ion mobility, and neurotransmitter cycling. Carbohydrates therefore significantly affect brain energy metabolism, emotional

* Corresponding author. *E-mail address:* akawsarabe@yahoo.com or akawsar@cu.ac.bd (Sarkar M.A. Kawsar)

stability, and cognitive function [9]. In addition to improving pharmacokinetic properties and promoting intermolecular interactions, carbohydrates are adaptable building blocks that enable a variety of derivatization processes [10]. In light of these findings, the current study investigated a number of D-glucofuranose derivatives that have demonstrated anticancer, antibacterial, and antidiabetic properties in both computational and experimental investigations. Nearly all of these substances have very low levels of toxicity, and several have demonstrated potent antipyretic and anti-inflammatory properties [11]. Using a variety of acylating agents, we were able to acylate 1,2:5,6-di-*O*-isopropylidene-α-D-glucofuranose selectively and produce the corresponding 3-*O*-acyl derivatives in respectable yields [12]. D-glucofuranose derivatives are strongly support the logical development of new antidiabetic drugs against human glucokinase [13].

The modified derivatives were designed by computational methods to explore their biological potential. Molecular docking was used to examine the binding affinities, hydrogen bonds and structural properties against the receptor human glucokinase (PDB IDs: 3IMX, 1V4S) [14]. Frontier molecular orbital (FMO) computations and density functional theory (DFT) provide information about compounds stability, reactivity and electronic structure. Additionally, the distribution of electron density on the surface of D-glucofuranose derivatives is revealed by molecular electrostatic potential (MEP) calculations, which is connected to how these compounds interact with biological targets and affect their pharmacological activity [15]. To assess the drug-likeness and pharmacokinetic features of protected carbohydrate scaffolds, which are frequently favorable, according to these predictive models ADMET predictions are frequently included into computational workflows [16]. To evaluate the potential antibacterial, antiviral, anti-inflammatory and anti-carcinogenic activities of the derivatives PASS is used [17]. Natural Bond Orbital (NBO) analysis is used in studies to clarify the fundamental chemical and physical properties of these compounds [18]. The purpose of this work is to use computational methods to integrate D-glucofuranose derivatives as potential inhibitors and modulators of human glucokinase and its isoforms [19].

Type 2 diabetes mellitus (T2DM) is a long-term metabolic disorder characterized by elevated blood glucose levels. To effectively treat diabetes mellitus (T2DM), maintaining glycemic control and maintaining functional pancreatic β-cell activity [20]. It was projected that 463 million people aged 20–79 years, representing 9.3% of the world's adult population had diabetes in 2019.

By 2030, this figure is expected to increase to 578 million, or 10.2% of the global adult population, and by 2045, it will have grown to 700 million, or 10.9% of the global adult population [21]. In recent years, the antidiabetic target glucokinase aids in managing type 2 diabetes by reducing blood glucose levels and enhancing glucose metabolism [22]. To evaluate the binding potential of D-glucofuranose derivatives and gain insight into their potential antidiabetic activity, structural conformations from both the active closed (3IMX) and inert super-open (1V4S) states were used. The generated activity map contains 97% of all possible single amino acid variations, and activity scores are linked to fasting glucose levels in people with GCK mutations, in vitro catalytic yield, and evolutionary conservation [23]. These structures also revealed an allosteric region, which allows tiny compounds to influence the enzymes kinetic characteristics. This discovery established the molecular basis for activating human glucokinase (PDB IDs: 3IMX, 1V4S), a potential treatment strategy for type 2 diabetes mellitus [24]. Using molecular docking and *in silico* studies, the purpose of this study was to examine the binding interactions and antidiabetic potential of D-glucofuranose derivatives (**2-9**) against human glucokinase (3IMX, 1V4S).

2. Computational details

2.1. Computational approaches

The Gaussian 09W program package was used to optimize the 3D structure of D-glucofuranose derivatives. First, the optimum structure was utilized by DFT and the B3LYP theoretical technique using 6-31G (d,p) basis set to investigate the electronic and thermal properties [25]. Dipole moments, polarizabilities, first-order hyperpolarizabilities, and optimal molecular structures were calculated for each molecule. In addition, quantum chemical descriptors such as chemical potential (μ), electronegativity (χ), chemical hardness (η), softness (S), and electrophilicity (ω) were examined. The FMOs were analyzed using HOMO and LUMO energies. MEP surfaces and NBO charges were also analyzed [26]. Additionally, protein-ligand binding energies and identifying ligand binding sites and interactions in the target protein, one of the most often used molecular modeling techniques is docking. The molecules that are highly active for the specified target protein are found using this energy which is performed by AutoDock Vina [27]. The selected crystal structure of proteins (3IMX, 1V4S) provides access to the PDB information via its RCSB.org research-focused website [28]. The energy of the proteins was minimized by the Swiss PDB viewer and the residues. Identification of the type of interaction and bond distances between the active sites in the target and ligand conformation is aided by the Discovery Studio [29]. Docking ligand input files are created with AutoDock Tools then saved as pdbqt files. The ADMET module allows the retrieval of drug discovery and biological information about compounds using standard SMILES notation. It is supported by the main database of admetSAR3.0 [30]. PASS Online, an open-access web resource is intended to predict the biological activity profiles of organic compounds using their structural formulas, covering more than 4,000 different types of bioactivities with an average accuracy greater then 95% [31].

The 2D structures of D-glucofuranose (**1**) and its derivatives (**2-9**) (Figure 1) presented in this work were created with ChemDraw 2.0 software.

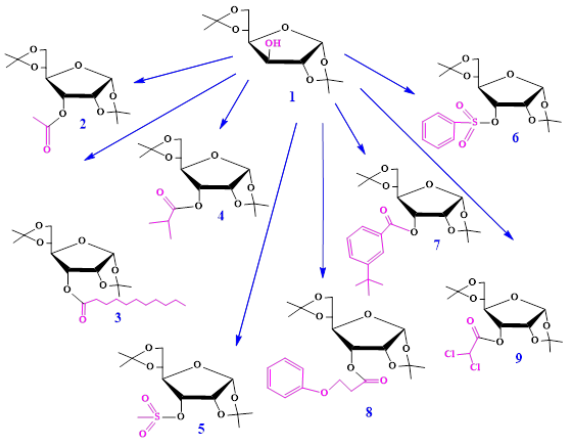

Figure 1. 2D structures of D-glucofuranose (**1**) and its derivatives (**2-9**)

3. Results and discussion

3.1. Optimized geometry

The newly synthesized derivatives of D-glucofuranose applied in the present study were designated according to the reaction scheme. In most quantum chemical calculations, the first step is geometry optimization [32]. The density functional theory (DFT) method with the B3LYP/631-G (d,p) basis set was applied to analyze the title compound's optimal molecular structure reported in Table 1, vibrational analysis, and electronic characteristics [33].

Table 1. Optimized structure of D-glucofuranose (**1**) and its derivatives (**2-9**)

Compound No.	Optimized structure	Compound No.	Optimized structure
1	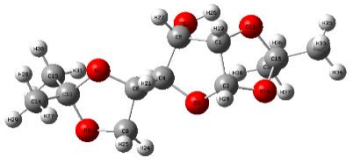	**2**	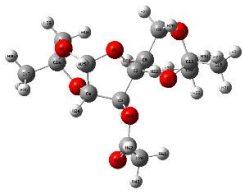
3	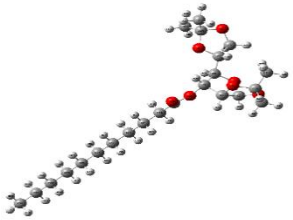	**4**	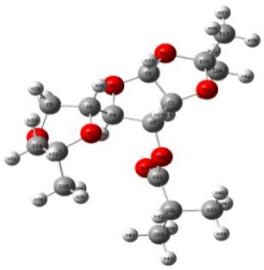
5	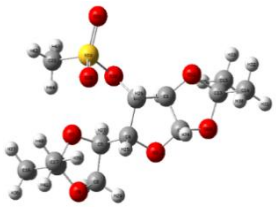	**6**	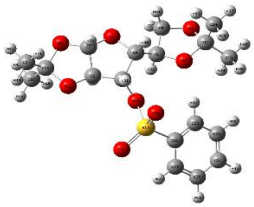
7	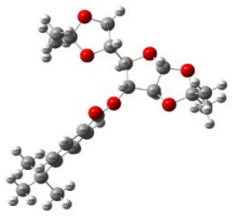	**8**	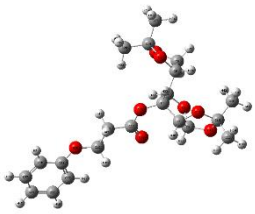
9	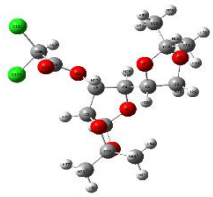		

HOMO and LUMO theoretical computations are often performed using an *ab initio* approach and density functional theory (DFT). To determine distinct charge distribution zones in each of the five molecules, the electrostatic potential maps (EPMs), chemical hardness (η), electronegativity (χ), and quantum chemical potential (μ) are also computed [34]. A proper design phase improves the efficacy of structure-based optimization and molecular docking.

3.2. Thermodynamic analysis

The thermodynamic properties characterize the energy content of a system. The thermodynamic parameters of a system in thermal equilibrium can be measured to evaluate the ligand-protein complexes strength and stability [35]. The enthalpy, entropy, Gibbs free energy, internal energy and dipole moment are the most common thermodynamic parameters [36].

Table 2 displays the stoichiometry, electronic energy, enthalpy, Gibb's free energy, dipole moment and polarizability of the D-glucofuranose derivatives. One can predict the inherent spontaneity of a reaction and the stability of the formed product by examining the enthalpy and free energy numbers. A higher electrical energy value increases the likelihood of achieving thermal stability. The dipole moment also impacts noncovalent interactions and the formation of hydrogen bonds in drug design. A greater dipole moment, in contrast can enhance the ligand binding capability. Covalent bond formation is more likely when polarizability is present [37]. It has been noted that compound **6** has a greater dipole moment (3.9801 D) than any other derivatives. Out of all derivatives, compound **3** (0.652444 Hartree**)** has the highest electronic energy. All the derivatives have larger absolute energies than the parent ligand (**1**). Furthermore, all aromatic D-glucofuranose derivatives demonstrated significantly increased polarizability. As a result, this discussion demonstrated that modifying the hydroxyl (-OH) groups of the derivatives considerably enhances their thermodynamic characteristics, highlighting the inherent stability of the produced derivatives. The physicochemical parameters have the highest polarizability value (260.63 a.u.) among all the derivatives. The presence of bulky acylating groups suggested at an enhancement in polarizability. However, it can be revealed that all of these produced D-glucofuranose derivatives are potentially more stable than their parent structure.

Table 2. The electronic energy, enthalpy, Gibbs free energy, dipole moment and polarizability of D-glucofuranose (**1**) and its derivatives (**2-9**)

Compound No.	Stoichiometry	Electronic energy (Hartree)	Enthalpy (Hartree)	Gibbs free energy (Hartree)	Dipole moment (D)	Polarizability (a.u.)
1	$C_{12}H_{20}O_6$	0.340296	0.341240	0.276792	2.7831	138.54
2	$C_{14}H_{22}O_7$	0.381508	0.382452	0.307174	1.7292	161.03
3	$C_{23}H_{40}O_7$	0.652444	0.653388	0.546064	2.0028	260.55
4	$C_{16}H_{26}O_7$	0.441378	0.442322	0.362295	2.9182	182.22
5	$C_{13}H_{22}O_8S$	0.380749	0.381703	0.304753	3.9571	182.02
6	$C_{18}H_{24}O_8S$	0.437479	0.438423	0.352480	3.9801	231.64
7	$C_{23}H_{32}O_7$	0.557253	0.558197	0.463097	3.2501	260.63
8	$C_{21}H_{28}O_8$	0.503817	0.504761	0.411999	1.5783	234.16
9	$C_{14}H_{20}O_7Cl_2$	0.364854	0.365798	0.282822	2.6175	179.88

3.3. Frontier molecular orbitals (FMOs)

Frontier molecular orbitals (FMOs), namely the HOMO and LUMO, are crucial for determining chemical reactivity and the degree to which a drug binds to a specific molecular receptor [38]. Table 3 displays the title compound and its derivatives HOMO-LUMO plot.

Table 3. Molecular orbitals (HOMO-LUMO) of D-glucofuranose (**1**) and its derivatives (**2-9**)

Compound No.	HOMO	LUMO
1	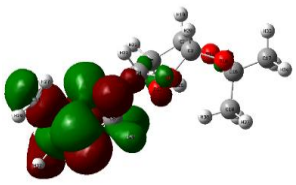	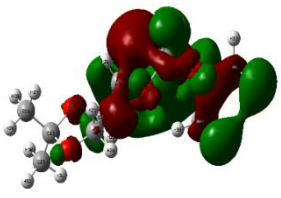
2	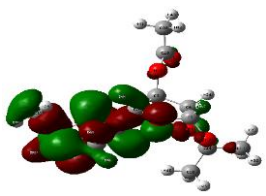	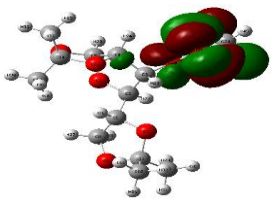

Compound No.	HOMO	LUMO
3	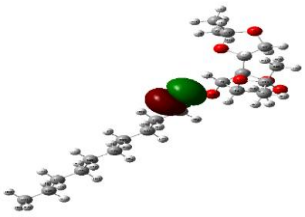	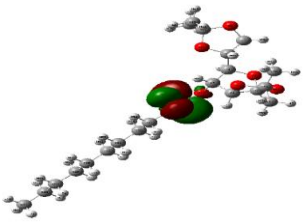
4	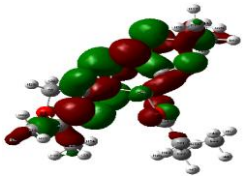	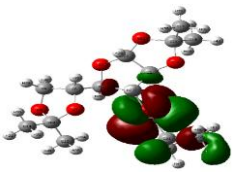
5	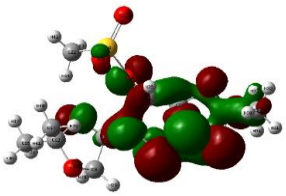	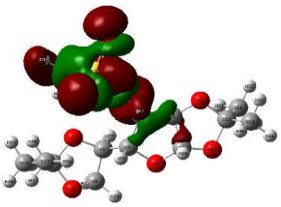
6	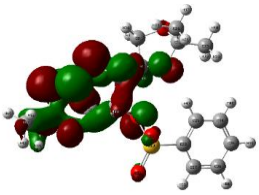	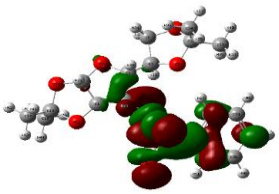
7	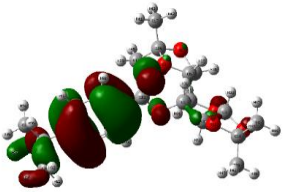	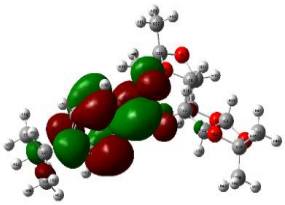
8	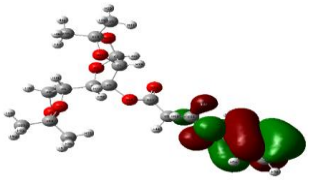	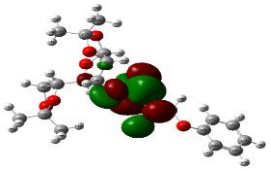
9	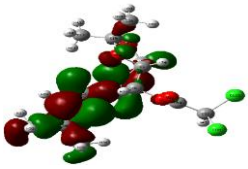	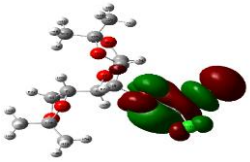

The kinetic and chemical stability of a molecule are predicted by the energy difference between its HOMO and LUMO [39]. A molecule with a small gap between frontier orbitals is highly polarizable and generally associated with low kinetic stability and elevated chemical reactivity. Since these electrons tend to be an electron donor, the ionization potential is directly correlated with the energy of the HOMO, which can be thought of as the outermost orbital that holds electrons. However, the LUMO energy is directly correlated with the electron affinity, thus the LUMO can take up electrons [40]. The density of states (DOS) plot was generated to analyze the highest and lowest energy gaps of the modified derivatives, which are useful for understanding electronic structure and determining the resultant stability and reactivity. The HOMO–LUMO energy gap ($\Delta E = E\_LUMO - E\_HOMO$) of compound **6** exhibits a shorter HOMO–LUMO gap (0.1697 eV) than compound **2** (0.2436 eV), suggesting higher chemical reactivity and the possibility of a stronger interaction with the target protein, according to the DOS plots of compounds **2** and **6** (Figure 2).

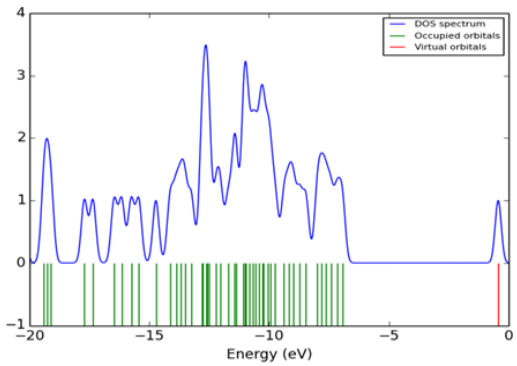

a.

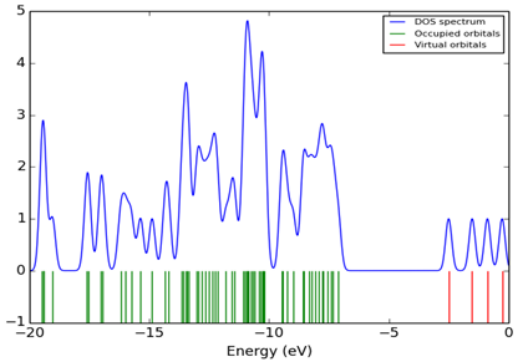

b.

Figure 2. DOS diagrams of compounds **3** (a) and **6** (b)

3.4. Global reactivity descriptors

Based on the HOMO-LUMO energy levels, several chemical reactivity characteristics were computed. Hardness (η), chemical potential (μ), softness (S), electronegativity (χ) and the electrophilicity index (ω) are examples of global chemical reactivity descriptors that have been computed using the HOMO and LUMO energy value of the compounds [41]. The electronic properties, chemical reactivity, and stability were all evaluated based on the energy gap (*ΔE*) of the Highest Occupied Molecular Orbital (HOMO) and Lowest Unoccupied Molecular Orbital (LUMO). Hardness (*η*), softness (*S*), and chemical potential (*μ*) were determined using the following formulas [42]:

$$\Delta E = (\varepsilon LUMO - \varepsilon HOMO) \quad (1)$$

$$\eta = \frac{(\varepsilon LUMO - \varepsilon HOMO)}{2} \quad (2)$$

$$S = \frac{1}{\eta} \quad (3)$$

$$\mu = \frac{(\varepsilon LUMO + \varepsilon HOMO)}{2} \quad (4)$$

The energies of the HOMO and LUMO, the HOMO–LUMO gap, chemical hardness, and softness of all ligands are presented in Table 4.

Table 4. Energy (eV) of the HOMO, LUMO, energy gap, hardness and softness, chemical potential, electronegativity, and electrophilicity of glucofuranose (**1**) and its derivatives (**2-9**)

Compound No.	εHOMO (eV)	εLUMO (eV)	Gap, ΔE (eV)	Hardness, η (eV)	Softness, S (eV^{-1})	Chemical potential, μ (eV)	Electronegativity, χ (eV)	Electrophilicity, ω (eV)
1	-0.2492	-0.0439	0.2931	0.1466	6.8213	0.1466	0.1027	0.0360
2	-0.2549	-0.0158	0.2391	0.1196	8.3612	-0.1354	0.1354	0.0766
3	-0.2729	-0.0293	0.2436	0.1218	8.2102	-0.1511	0.1511	0.0094
4	-0.2545	-0.0158	0.2386	0.1194	8.3752	-0.1352	0.1352	0.0765
5	-0.2637	-0.0896	0.1741	0.0871	11.4812	-0.1767	0.1767	0.1792
6	-0.2615	-0.0918	0.1697	0.0849	11.7786	-0.1767	0.1767	0.1839
7	-0.2525	-0.0518	0.2007	0.1004	9.9606	-0.1522	0.1522	0.1154
8	-0.2226	-0.0260	0.1966	0.0983	10.1730	-0.1243	0.1243	0.0786
9	-0.2625	-0.0809	0.1816	0.0908	11.0132	-0.1717	0.1717	0.1623

Among these compounds, compound **3** (the undecanoyl derivative) exhibits the highest HOMO–LUMO energy gap, indicating the highest stability and, consequently, the lowest chemical reactivity. In contrast, compound **6** (the benzenesulfonyl derivative) shows the lowest energy gap. Compound **2** displays the second-highest HOMO–LUMO gap, which gradually decreases for compounds **4** and **9**. Accordingly, the stability of compound **2** is the second highest and gradually decreases for compounds **4** and **5**, respectively. As compound **6** showed lowest HOMO-LUMO gap it showed lowest stability, i.e. highest chemical reactivity. Consequently, this compound showed lowest hardness (0.0849) and the highest softness (11.7786). Chemical hardness and softness are directly related to the energy gap between the HOMO-LUMO of a molecule. Analysis of the data showed that compound **6** has the lowest HOMO-LUMO gap and the highest softness, which may be potentially responsible for its higher chemical reactivity compared to the others. A reduced HOMO-LUMO gap in ligands and complexes enhances their softness, which makes them relatively more polarizable and chemically reactive compared to others [43].

3.5. Molecular electrostatic potential (MEP)

The molecular electrostatic potential (MEP) is commonly used as a reactivity map to illustrate the most probable region susceptible to electrophilic and nucleophilic attacks by charged point like reagents on organic molecules. It helps to interpret biological recognition mechanisms and hydrogen bonding interaction [44]. The MEP counter map gives a simple technique to predict how different shapes may interact. Different colors are used to represent the various electrostatic potential levels at the surface. The negative areas (red color) of the MEP were associated with electrophilic reactivity, the positive areas (blue color) were associated with nucleophilic reactivity, and the

green color represents zero potential areas [45] as illustrated in Figure 3. Using the B3LYP/6-31G basis set the molecular electrostatic potential (MEP) was generated [46]. Compound **6** (-6.370 e^{-2}) has a stronger negative potential than compound **9** (-4.799e^{-2}), according to MEP analysis, suggesting that a more prominent electron-rich site appropriate for electrophilic interactions.

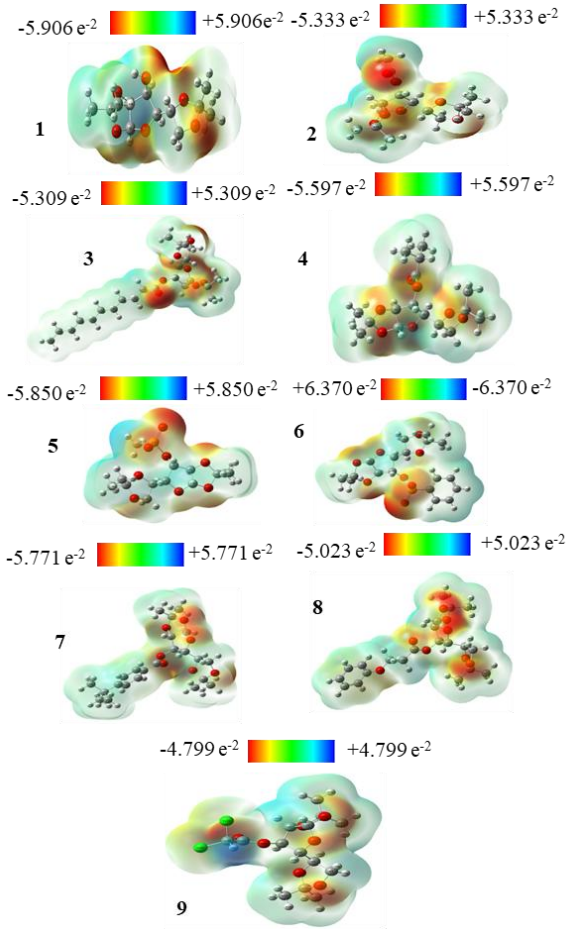

Figure 3. Molecular electrostatic potential map of glucofuranose (**1**) and its derivatives (**2-9**)

3.6. Natural bonding orbitals (NBOs) analysis

The NBO analysis offers a practical foundation for examining charge transfer or conjugative interactions in molecular systems, as well as an effective technique for examining intra and intermolecular interactions and bond connectivity [47]. It is also used to calculate changes in charge densities in proton donors and acceptors, specifically in bonding and antibonding orbitals. The NBO analysis successfully explains the rationalization of the H-bond. In general, hydrogen bonds are thought to form as a result of a hyperconjugative charge transfer interaction between the proton acceptor and the proton donor [48]. The dipole moment, molecular polarizations, and many other quantum characteristics of molecular systems can be predicted using the charges. The analysis of charge distribution points to donor-acceptor interactions and associated charge transfer within the molecule. By determining each atoms electron population as specified in the fundamental functions, Mulliken charges are computed. Figure 4 shows the charge distributions determined using the NBO and Mulliken using the B3LYP level with 6-31G (d,p) basis sets, which provides a more effective graphical representation of D-glucofuranose derivatives [48]. The NBO and Mulliken approaches anticipate that all of the H atoms in these derivatives will have positive charges; yet compound **7** has a higher partial positivity of H atoms.

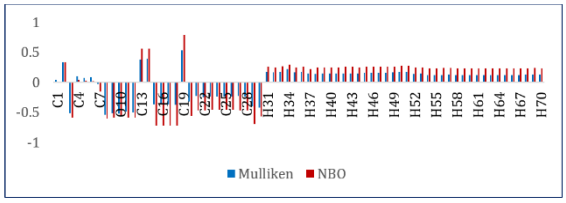

a.

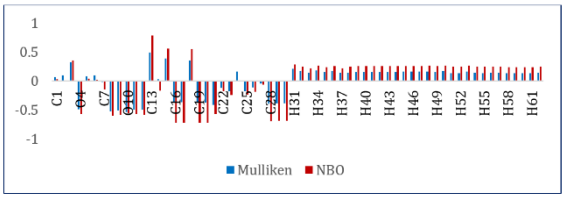

b.

Figure 4. Atomic partial charges of compounds **3** (a) and **7** (b)

3.7. Molecular docking and calculations of interactions

Molecular docking employs computational tools used to predict ligand binding affinity to receptor proteins [49]. This approach investigates the spatial and energetic compatibility of the ligand with the receptor active site, assisting in the identification of new drug candidates, refining current molecules and analyzing the complex interactions between drugs and receptors [50]. Molecular docking simulations were conducted using AutoDock Vina, where the drug was regarded as the ligand and the protein as the macromolecule. Both the macromolecule and ligand structures were prepared and saved in pdbqt format once docking was finished. This was done so that Discovery Studio (version 4.1) could examine and analyze the docking results and identify non-bonding interactions among the ligands and residues of amino acids [51] as shown in Table 5 and Table 6.

Table 5. Selected binding affinity (kcal/mol) and nonbonding interactions of D-glucofuranose (**1**) and its derivatives (**2-9**) with 3IMX

Human glucokinase (3IMX)				
Compound No.	**Binding affinity**	**Residues contacts**	**Distance**	**Types of bonds**
1	-6.1	ARG85	2.82484	Conventional Hydrogen Bond
		ASP409	2.70491	Conventional Hydrogen Bond
		SER445	2.60268	Conventional Hydrogen Bond
		ASP78	3.52565	Carbon Hydrogen Bond

Human glucokinase (3IMX)				
Compound No.	**Binding affinity**	**Residues contacts**	**Distance**	**Types of bonds**
		ILE225	5.40385	Alkyl group
		ARG85	4.84814	Alkyl group
2	-6.7	THR82	2.62447	Conventional Hydrogen Bond
		THR228	2.05903	Conventional Hydrogen Bond
		ASN83	3.46523	Carbon Hydrogen Bond
		ASN83	3.75083	Carbon Hydrogen Bond
		ARG85	4.07921	Alkyl group
		MET107	5.04141	Alkyl group
		ILE225	4.78822	Alkyl group
		ILE225	4.07662	Alkyl group
3	-7.4	SER69	1.90283	Conventional Hydrogen Bond
		TRP99	3.02808	Carbon Hydrogen Bond
		TYR214	3.63845	π-σ
		VAL452	5.34025	Alkyl group
		VAL455	5.35775	Alkylgroup
		VAL455	4.7757	Alkyl group
		VAL455	4.44575	Alkyl group
		ILE211	5.01011	Alkyl group
		LEU451	4.94836	Alkyl group
		ILE211	4.22434	Alkyl group
		MET210	4.92831	Alkyl group
		ILE211	4.24529	Alkyl group
		TRP99	4.56134	π-Alkyl
		TYR214	5.25479	π-Alkyl
		TYR214	5.40018	π-Alkyl
		TYR214	3.97999	π-Alkyl
		HIS218	4.57506	π-Alkyl
		HIS218	4.0405	π-Alkyl
4	-7.5	TYR215	3.7026	Carbon Hydrogen Bond
		HIS218	3.48047	Carbon Hydrogen Bond
		PRO66	3.53497	Carbon Hydrogen Bond
		ILE211	4.10425	Alkyl group
		VAL62	5.26245	Alkyl group
		ILE211	3.74668	Alkyl group
		VAL452	4.37861	Alkyl group
		LEU451	4.0593	Alkyl group
		VAL455	5.21096	Alkyl group
		TRP99	4.87661	π-Alkyl
		TYR214	4.42174	π-Alkyl
		HIS218	4.8825	π-Alkyl
5	-7.0	TRP99	2.2113	Conventional Hydrogen Bond
		TRP99	3.52881	π-σ
		HIS218	5.0557	π-Sulfur
		ALA454	4.43734	Alkyl group
		VAL91	3.83032	Alkyl group
		VAL91	4.27108	Alkyl group
		VAL101	5.03891	Alkyl group
		ILE211	3.93262	Alkyl group
		VAL455	3.64709	Alkyl group
		TRP99	4.07355	π-Alkyl
		TRP99	4.07454	π-Alkyl
		TRP99	4.75905	π-Alkyl
		TYR214	4.18190	π-Alkyl
		TYR215	4.38929	π-Alkyl
6	**-8.9**	HIS218	3.56891	Conventional Hydrogen Bond
		SER69	2.85366	Carbon Hydrogen Bond
		TYR214	5.82051	π-Donor Hydrogen Bond
		TYR215	5.12177	π-Sulfur
		HIS218	5.71121	π-Sulfur
		TRP99	4.91227	π-Sulfur
		TRP99	5.35615	π-π-T-shaped
		TYR215	5.27668	π-π-T-shaped
		VAL62	5.16822	π-π-T-shaped

Human glucokinase (3IMX)				
Compound No.	**Binding affinity**	**Residues contacts**	**Distance**	**Types of bonds**
		ILE211	3.84158	Alkyl group
		VAL452	4.8375	Alkyl group
		TYR214	4.38858	Alkyl group
		LEU451	5.07733	π-Alkyl
		ALA454	4.9876	π-Alkyl
7	**-9.0**	TYR214	2.57661	Conventional Hydrogen Bond
		HIS218	2.86079	Carbon Hydrogen Bond
		TRP99	3.60604	π-σ
		TRP99	5.32348	π-π-T-shaped
		TYR215	4.99453	π-π-T-shaped
		VAL91	3.90399	Alkyl group
		LEU451	5.40505	Alkyl group
		ILE211	3.91869	Alkyl group
		VAL452	4.23039	Alkyl group
		VAL455	4.60257	Alkyl group
		VAL62	5.14337	Alkyl group
		PRO66	4.61049	Alkyl group
		VAL452	5.03625	Alkyl group
		VAL455	3.85625	Alkyl group
		TRP99	4.67359	π-Alkyl
		TRP99	4.77968	π-Alkyl
		HIS218	5.36028	π-Alkyl
		LEU451	5.10105	π-Alkyl
8	-8.8	TRP99	2.10101	Conventional Hydrogen Bond
		TYR214	2.29874	Conventional Hydrogen Bond
		SER69	3.49678	Carbon Hydrogen Bond
		MET210	5.87597	π-Sulfur
		TYR214	3.80968	π-π-Stacked
		ILE211	5.05193	Alkyl
		LEU451	4.20286	Alkyl
		TRP99	4.43192	π-Alkyl
		TYR214	5.32301	π-Alkyl
		TYR215	5.47547	π-Alkyl
		HIS218	5.27759	π-Alkyl
		HIS218	4.95104	π-Alkyl
		ILE211	5.38483	π-Alkyl
		MET235	5.26589	π-Alkyl
9	-6.6	THR228	2.37149	Conventional Hydrogen Bond
		LYS169	5.46076	Alkyl group
		ILE225	5.25593	Alkyl group
		ARG85	4.5599	Alkyl group
		MET107	5.32325	Alkyl group
		ARG85	4.48993	Alkyl group
		MET107	4.98144	Alkyl group

Table 6. Selected binding affinity (kcal/mol) and nonbonding interactions of D-glucofuranose (**1**) and its derivatives (**2-9**) with 1V4S

Human glucokinase (1V4S)				
Compound No.	**Binding affinity**	**Residues contacts**	**Distance**	**Types of bonds**
1	-5.9	ARG63	2.68201	Conventional Hydrogen Bond
		VAL62	4.6504	Alkyl group
		VAL452	4.02816	Alkyl group
		VAL455	3.95159	Alkyl group
		VAL62	4.13925	Alkyl group
		ILE159	3.82814	Alkyl group
		VAL452	4.80364	Alkyl group
		TYR61	4.86249	π-Alkyl
2	-6.6	GLY81	2.91789	Conventional Hydrogen Bond
		SER411	1.96854	Conventional Hydrogen Bond
		GLY227	3.65871	Carbon Hydrogen Bond
3	-6.6	GLY299	2.72662	Conventional Hydrogen Bond
		GLU300	2.53088	Conventional Hydrogen Bond
		THR332	2.81551	Conventional Hydrogen Bond
		ARG333	3.04765	Conventional Hydrogen Bond

Human glucokinase (1V4S)				
Compound No.	**Binding affinity**	**Residues contacts**	**Distance**	**Types of bonds**
		GLY295	3.5739	Carbon Hydrogen Bond
		ARG327	4.63925	Alkyl group
		ARG333	4.3716	Alkyl group
		ARG333	4.17778	Alkyl group
		VAL277	4.38549	Alkyl group
4	-6.6	ARG85	2.57804	Conventional Hydrogen Bond
		ARG85	2.4134	Conventional Hydrogen Bond
		THR228	2.71183	Conventional Hydrogen Bond
		SER411	1.97503	Conventional Hydrogen Bond
		GLY227	3.7919	Carbon Hydrogen Bond
		ASP78	3.49962	Carbon Hydrogen Bond
		LYS169	5.29962	Alkyl group
		ILE225	4.92491	Alkyl group
		LYS169	4.54746	Alkyl group
5	-6.6	ARG85	2.04782	Conventional Hydrogen Bond
		ARG85	2.39423	Conventional Hydrogen Bond
		THR228	2.09516	Conventional Hydrogen Bond
		SER411	2.82668	Conventional Hydrogen Bond
		SER445	2.88387	Conventional Hydrogen Bond
		LYS169	5.40084	Alkyl group
		ILE225	4.7526	Alkyl group
		LYS169	4.82264	Alkyl group
		LYS414	4.50264	Alkyl group
6	-7.2	LYS169	2.33636	Conventional Hydrogen Bond
		THR228	2.31582	Conventional Hydrogen Bond
		GLY81	3.5503	Carbon Hydrogen Bond
		ASP205	3.32895	π-Anion
		ILE225	5.05272	π-Alkyl
7	**-8.2**	VAL455	3.55115	π-σ
		LYS459	4.75827	Alkyl group
		VAL62	5.38854	Alkyl group
		PRO66	5.45842	Alkyl group
		ILE211	5.06509	Alkyl group
		VAL455	4.3068	Alkyl group
		PRO66	4.7743	Alkyl group
		VAL62	4.77884	π-Alkyl
		PRO66	4.82687	π-Alkyl
		VAL452	4.75969	π-Alkyl
		ALA456	5.40973	π-Alkyl
8	**-7.3**	SER64	2.61087	Conventional Hydrogen Bond
		ARG250	2.8894	Conventional Hydrogen Bond
		ARG250	2.58697	Conventional Hydrogen Bond
		ARG250	3.63882	Carbon Hydrogen Bond
		ILE211	3.64251	π-σ
		TYR214	4.96202	π-π-T-shaped
9	-6.4	GLY81	2.88541	Conventional Hydrogen Bond
		ARG85	2.7752	Conventional Hydrogen Bond
		ARG85	2.61418	Conventional Hydrogen Bond
		SER411	1.97848	Conventional Hydrogen Bond
		GLY227	3.52688	Carbon Hydrogen Bond

We have employed two distinct human glucokinase receptors (PDB: 3IMX and 1V4S) from the Protein Data Bank [52]. According to the results of the docking analysis, all compounds including the parent chemical, have binding affinities between -6.1 and -9.0 kcal/mol and -5.9 and -8.2 kcal/mol. The grid box size for receptor 3IMX is (51.611, 55.76, 73.61) with the (x, y, z) directions set to these values, while for 1V4S, it is (58.76, 71.37, 60.74). As shown below, compounds **7** and **6**, in the case of 3IMX and compounds **7** and **8**, in the case of 1V4S, showed the highest binding affinities compared to the parent D-glucofuranose compound. These results indicated that modification of the -OH group of D-glucofuranose increased the binding affinity [53]. The docked conformation clearly showed how the therapeutic molecules bind to the human glucokinase receptors (3IMX and 1V4S) macromolecular structure (Figure 5 and 6).

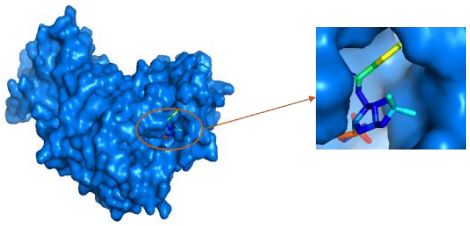

Figure 5. Docked pose of compound **7** at the inhibition binding site of 3IMX

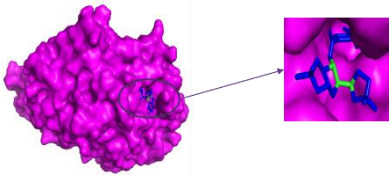

Figure 6. Docked pose of compound (**7**) at the inhibition binding site of 1V4S

From the post-docking study, it was observed that compound **7** showed π-alkyl interactions with TRP99, LEU451, HIS218 (higher distance 5.36028 Å) in the active site of 3IMX and VAL62, ALA456, VAL452 (shorter distance 4.75969), PRO66 with 1V4S. Compounds **6** and **8** showed conventional hydrogen bonds with residues HIS218, SER64, ARG250, besides other interactions such as carbon-hydrogen bonds SER69, ARG250 and hydrophobic interactions such as pi-pi T shaped for TRP99, TYR214. Compounds **6** and **7** displayed the maximum π-π interactions with the TRP99 residue in 3IMX and compound 8 displayed maximum interactions with the TYR214 residue in 1V4S, denoting the tight binding with the active site. These results demonstrate that aromatic substituents can readily improve the binding and antiviral properties of their high electron density. Non-bonding interactions are shown in (Figure 7 and 8).

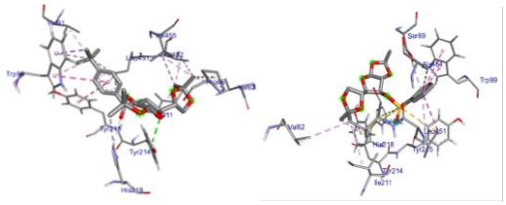

Figure 7. Nonbonding interactions of compounds **7** and **6**

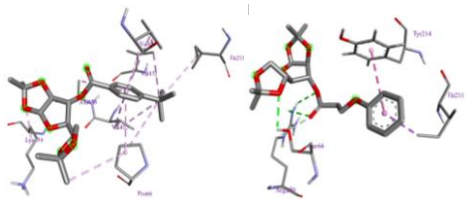

with 3IMX

Figure 8. Nonbonding interactions of compounds (**7** and **8**) with 1V4S

All of the analogs showed the highest π-π interactions with the TRP99 indicating a tight binding with the active site, in addition to HIS218. Due to strong hydrogen bonding, the binding energy and binding mode of those analogs were enhanced [54]. For compounds **4**, **5**, and **8**, the highest number of H-bonds was achieved when receptor 1V4S formed with GLY227, PRO66, and ASP78. (Figure 9 and 10) shows the hydrogen bond surface compounds (**7, 6**) and **(7, 8**), (Figure 9 and 10) show the hydrophobic surface compounds (**7, 6**) and (**7, 8**) with both glucokinase proteins. The analysis revealed that D-glucofuranose derivatives interact with the active site of the human glucokinase receptors 3IMX and 1V4S. Although blind docking studies suggest that all molecules have potential antidiabetic activity, compound **7**, bearing a 4-*t*-butylbenzoyl chloride aromatic substituent , the blind docking studies suggest that all the molecules have the potential to act as an effective agent substituent in the structure , exhibits the highest electron density and the most favorable minimum binding energy (−9.0 kcal/mol), indicating it as the most promising therapeutic candidate among the studied derivatives for the treatment of diabetes mellitus [55].

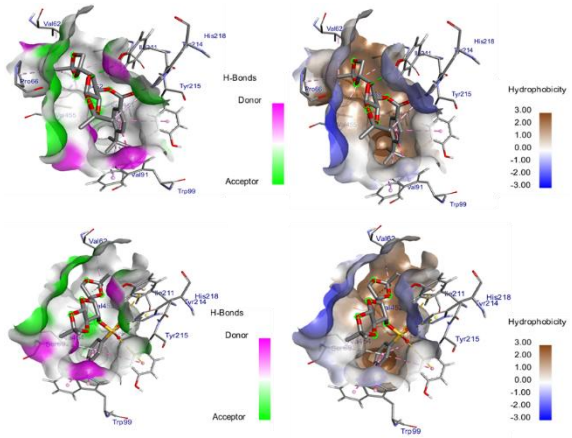

Figure 9. Hydrogen bonds (**a**) and hydrophobicity (**b**) of compounds **7** and **6** with 3IMX

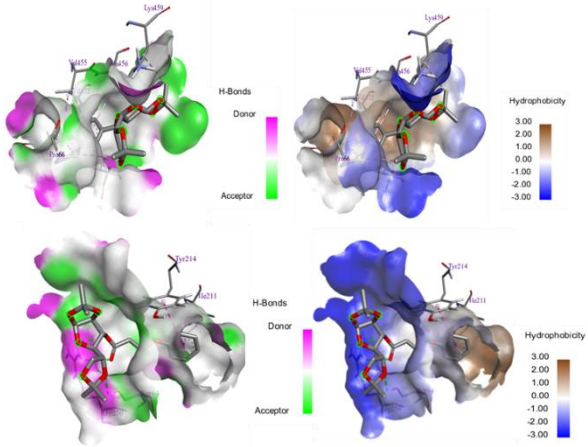

Figure 10. Hydrogen bonds (**c**) and hydrophobicity (**d**) of compounds (**7** and **8**) with 1V4S

3.8. ADMET analysis

Although carbohydrates are not toxic, D-glucofuranose derivatives (modified carbohydrates) contain toxicity. To predict an attempt of pharmacokinetic features such as the absorption, distribution, metabolism, excretion and toxicity (ADMET) of the compounds, the pkCSM web server was used [56]. Various pharmacokinetic and pharmacodynamic parameters, including human intestinal absorption, blood-brain barrier, cytochrome P450 inhibition, human ether-a-go-go-related genes

inhibition, and acute oral toxicity and rat acute toxicity [57] were evaluated and are summarized in Table 7.

Table 7. Selected pharmacokinetic properties of D-glucofuranose (**1**) and its derivatives (**2-9**)

Compound No.	BBB (log BB)	CYP2C19 inhibitor (Yes/No)	Intestional absorption (Human) (% Absorbed)	P-glyco protein inhibitor (Yes/No)	Water solubility	Oral rat acute toxicity LD50	hERG inhibitor (Yes/NO)
1	-0.282	No	100	No	-2.282	2.331	No
2	0.81	No	88.492	No	-3.927	2.482	No
3	-0.977	No	95.168	Yes	-4.9	2.118	No
4	0.775	No	85.875	No	-3.456	2.482	No
5	-1.183	No	98.750	Yes	-3.018	2.520	No
6	0.808	No	82.360	No	-3.037	2.482	No
7	-0.74	Yes	96.072	Yes	-5.237	2.537	No
8	-1.065	No	97.881	Yes	-4.339	3.060	No
9	-1.132	No	96.810	No	-3.585	2.871	No

All the compounds exhibited positive values (above the prescribed threshold, suggesting good permeability) with high probabilities, particularly regarding the blood-brain barrier and human intestinal absorption. Furthermore, modifications of D-glucofuranose yielded an inhibitor of P-glycogen. The analysis identified that **5**, **8**, **9** and **7** were potential inhibitor compounds that have high calculated values of intestinal absorption by humans, including over 80%. This suggests that the intestines may readily absorb these molecules and allow them to circulate in the bloodstream [58]. All tested compounds displayed an oral toxicity profile. Compound 8 showed the maximum LD_{50} value in rat acute toxicity evaluations compared to most of the compounds like **8**, **7** and **6** which demonstrate more toxicity with respect to parent D-glucofuranose. Since inhibition of hERG may cause long QT syndrome, additional studies are necessary to thoroughly evaluate the safety profile.

3.9. PASS prediction

The prediction of activity spectra for substances (PASS) serves as a software tool for evaluating the overall biological potential of organic drug-like molecules. PASS provides simultaneous predictions of various types of biological activities on the basis of the structure of organic compounds [59]. Pass prediction was performed *via* an online server (Way2Drug - main). This server presents the user with a list of numbers from zero to one, where "Pa" means "to be biologically active" and "Pi" means "to be biologically inactive." Thus, PASS can be employed to predict the biological activity profiles of virtual molecules before their chemical synthesis and experimental testing [60]. All of the D-glucofuranose compounds exhibited a variety of metabolic activities during our investigation, as expected by PASS, as shown in Table 8.

Table 8. Prediction of antiviral, antimicrobial and anticarcinogenic activity of D-glucofuranose (**1**) and its derivatives (**2-9**)

Compound No.	Antibacterial		Anticarcinogenic		Antifungal		Anti-inflammatory	
	Pa	**Pi**	**Pa**	**Pi**	**Pa**	**Pi**	**Pa**	**Pi**
1	0.497	0.017	0.368	0.037	0.552	0.023	0.962	0.003
2	0.512	0.015	0.388	0.033	0.632	0.015	0.957	0.004
3	0.497	0.017	0.359	0.039	0.665	0.013	0.943	0.004
4	0.525	0.014	0.288	0.063	0.660	0.012	0.942	0.004
5	0.370	0.038	0.298	0.059	0.366	0.058	0.944	0.004
6	0.318	0.054	0.188	0.134	0.319	0.074	0.923	0.004
7	0.413	0.027	0.335	0.046	0.598	0.019	0.939	0.004
8	0.409	0.028	0.298	0.059	0.587	0.020	0.921	0.004
9	0.476	0.019	0.217	0.104	0.539	0.025	0.984	0.004

All of these derivatives have antifungal properties, according to our research. Derivatives 3 and 4 had the highest Pa values, at 0.665 and 0.660, respectively. These chemicals are all anti-inflammatory and anticarcinogenic. The greatest values for both anti-inflammatory and anticarcinogenic properties were found for compounds **9** and **1** (0.984 and 0.962, respectively). Compound **2** has an outstanding Pa value of 0.388 due to its anticarcinogenic qualities, and compound **4** has a Pa value of 0.525 for its antibacterial qualities.

4. Conclusions

In the present study, a set of D-glucofuranose derivatives were analyzed through computational approaches to investigate their structural, electronic and binding properties as potential antidiabetic agents. The stability and electronic structure of the investigated compounds were determined *via* DFT calculations. Compound **6** has a greater dipole moment (3.9801 D), and compound **3** (0.652444 Hartree) has the highest electronic energy. The electronic property analysis confirmed the stability, charge distribution, and reactivity of the compounds by the HOMO–LUMO

gaps. Compound **6** presented a shorter HOMO–LUMO gap (0.1697 eV) than did compound **3** (0.2436 eV), which presented a greater HOMO–LUMO gap, suggesting greater chemical reactivity and the possibility of a stronger interaction with the target protein. These findings emphasize the significance of substituent effects on overall molecular behavior, which influences both binding efficiency and electrical properties properties. These derivatives exhibit favorable electronic transitions and strong intermolecular interactions, demonstrating both stability and biological significance. The docking analysis findings showed that each derivative favors favorable interactions with the human glucokinase active sites 3IMX and 1V4S. On the other hand, compound **7** had the highest binding affinity because of its aromatic group (4-*t*-butylbenzoyl chloride). The stability and reactivity of the compounds under investigation were validated with electronic property tests, which suggested that they would be good therapeutic candidates. Among the derivatives under study, compound **7** presented the greatest binding energy (-9.0 kcal/mol), suggesting that it has significant potential as a lead chemical. These findings highlight the potential of D-glucofuranose derivatives in the development of innovative therapeutic drugs for the treatment of diabetes.

Acknowledgements

The work has been supported by the Ministry of Science and Technology (MoST) of the Peoples Republic of Bangladesh (No. SRG-256652) (2025-2026).

Conflict of interest

Authors declare no conflict of interest.

References

[1]. J.H. Cummings, A.M. Stephen, Carbohydrate terminology and classification, European Journal of Clinical Nutrition 61 (2007) S5-S18. DOI: 10.1038/SJ.EJCN.1602936

[2]. J. Agirre, G.J. Davies, K.S. Wilson, K.D. Cowtan, Carbohydrate structure: the rocky road to automation, Current Opinion in Structural Biology 44 (2017) 39-47. DOI: 10.1016/j.sbi.2016.11.011

[3]. L. Su, Y. Feng, K. Wei, X. Xu, R. Liu, G. Chen, Carbohydrate-Based Macromolecular Biomaterials, Chemical Reviews 121 (2021) 10950-11029. DOI: 10.1021/ACS.CHEMREV.0C01338

[4]. M. Arifuzzaman, M.M. Islam, M.M. Rahman, M.A. Rahman, S.M.A. Kawsar, An efficient approach to the synthesis of thymidine derivatives containing various acyl groups: Characterization and antibacterial activities, Acta Pharmaceutica Sciencia 56 (2018) 7–22. DOI: 10.23893/1307-2080.APS.05622

[5]. S.M.A. Kawsar, R. Matsumoto, Y. Fujii, Y. Yasumitsu, C. Dohgasaki, M. Hosono, K. Nitta, J. Hamako, T. Matsui, K. Noriaki, Y. Ozeki, Purification and biochemical characterization of a D-galactose binding lectin from Japanese sea hare (*Aplysia kurodai*) eggs, Biochemistry 74 (2009) 709-716. DOI: 10.1134/S0006297909070025

[6]. S.M.A. Kawsar, E. Huq, N. Nahar, Cytotoxicity assessment of the aerial parts of *Macrotyloma uniflorum* Linn, International Journal of Pharmacology 4 (2008) 297-300. DOI: 10.3923/ijp.2008.297.300

[7]. S.M.A. Kawsar, G. Mostafa, E. Huq, N. Nahar, Y. Ozeki, Chemical constituents and hemolytic activity of *Macrotyloma uniflorum* L., International Journal of Biological Chemistry 3 (2009) 42-48. https://scialert.net/abstract/?doi=ijbc.2009.42.48

[8]. P. Weller, Carbohydrates: Structure, function, and importance in human health, Journal of Nutrition & Food Sciences 14 (2024) 100050. DOI: 10.35248/2155-9600.24.14.50

[9]. M.T. Arshad, S. Maqsood, R. Altalhi, G. Shamlan, I.A.M. Ahmed, A. Ikram, M.A. Abdullahi, Role of dietary carbohydrates in cognitive function: A review, Food Science & Nutrition 13 (2025) 70516. DOI: 10.1002/FSN3.70516

[10]. J.P.B. Lopes, L. Silva, D.S. Lüdtke, An overview on the synthesis of carbohydrate-based molecules with biological activity related to neurodegenerative diseases, RSC Medicinal Chemistry 12 (2021) 2001-2015. DOI: 10.1039/D1MD00217A

[11]. A. Goi, T. Bruzzese, A.F. Notarianni, M. Riva, A. Ronchini, Synthesis and pharmacological properties of 3-*O*-derivatives of 1,2,5,6-di-*O*-isopropylidene-alpha-D-glucofuranose, Arzneimittel-Forschung 29 (1979) 986. DOI: 10.1002/CHIN.197944341

[12]. M. Islam, A. Zzaman, M. Rahman, M.A. Rahman, S. Mohammad, S.M.A. Kawsar, Novel methyl 4,6-*O*-benzylidene-α-D-glucopyranoside derivatives: Synthesis, structural characterization and evaluation of antibacterial activities, Hacettepe Journal of Biology and Chemistry 47 (2019) 153-164. DOI: 10.15671/HJBC.622038

[13]. A. Ali, Development of antidiabetic drugs from benzamide derivatives as glucokinase activator: A computational approach, Saudi Journal of Biological Sciences 29 (2022) 3313-3325. DOI: 10.1016/J.SJBS.2022.01.058

[14]. M.R. Hossain, S.M.A. Kawsar, TD-DFT, Vibrational spectra, molecular docking, ADMET, and PASS assessment as potential inhibitors of SARS-CoV-2 alpha and beta variants of uridine derivatives, Physical Chemistry Research 13 (2025) 643-668. DOI: 10.22036/pcr.2025.513955.2661

[15]. S.M.A. Kawsar, M.A. Hosen. An optimization and pharmacokinetic studies of some thymidine derivatives, Turkish Computational and Theoretical Chemistry, 4 (2020), 59-66. DOI: 10.33435/tcandtc.718807

[16]. M.F. Labib, S. Saha, S.M.A. Kawsar, Quantum computational, molecular docking, dynamics, PASS, and ADMET analyses of methyl α-D-glucopyranoside derivatives, Physical Chemistry

Research 13 (2025) 381-400. DOI: 10.22036/PCR.2025.491267.2601

[17]. N. Akter, L. Bourougaa, M. Ouassaf, R.C. Bhowmic, K.M. Uddin, A.R. Bhat, S. Ahmed, S.M.A. Kawsar, Molecular docking, ADME-Tox, DFT and molecular dynamics simulation of butyroyl glucopyranoside derivatives against DNA gyrase inhibitors as antimicrobial agents, Journal of Molecular Structure 1307 (2024) 137930. DOI: 10.1016/J.MOLSTRUC.2024.137930

[18]. F. Yasmin, M.R. Amin, M.A. Hosen, M.Z.H. Bulbul, S. Dey, S.M.A. Kawsar, Monossacharide derivatives; synthesis, antimicrobial, PASS, antiviral and molecular docking studies against SARS-CoV-2 Mpro inhibitors, Cellulose Chemistry and Technology 55 (2021) 477-499. DOI: 10.35812/CelluloseChemTechnol.2021.55.44

[19]. A.K.M.S. Kabir, S.M.A. Kawsar, M.M.R. Bhuiyan, Md. S. Rahman, M.E. Chowdhury, Antimicrobial screening of some derivatives of methyl α-D-glucopyranoside, Biological Sciences – PJSIR 52 (2009) 138-142. https://www.biostaging.pjsir.org/index.php/biological-sciences/article/view/536

[20]. D. Haddad, V.S. Dsouza, F. Al-Mulla, A. Al Madhoun, New-generation glucokinase activators: Potential game-changers in type 2 diabetes treatment, International Journal of Molecular Sciences 25 (2024) 572. DOI: 10.3390/IJMS25010571

[21]. M.Z. Banday, A.S. Sameer, S. Nissar, Pathophysiology of diabetes: An overview, Avicenna Journal of Medicine 10 (2020) 174-188. DOI: 10.4103/AJM.AJM5320

[22]. Y. Ren, L. Li, L. Wan, Y. Huang, S. Cao, Glucokinase as an emerging anti-diabetes target and recent progress in the development of its agonists, Journal of Enzyme Inhibition and Medicinal Chemistry 37 (2022) 606-615. DOI: 10.1080/14756366.2021.2025362

[23]. Y. Abu Aqel, A. Alnesf, I.I. Aigha, Z. Islam, P.R. Kolatkar, A. Teo, E.M. Abdelalim, Glucokinase (GCK) in diabetes: from molecular mechanisms to disease pathogenesis, Cellular and Molecular Biology Letters 29 (2024) 120. DOI: 10.1186/S11658-024-00640-3

[24]. K. Kamata, M. Mitsuya, T. Nishimura, J.I. Eiki, Y. Nagata, Structural basis for allosteric regulation of themonomeric allosteric enzyme human glucokinase, Structure 12 (2004) 429–438. DOI: 10.1016/J.STR.2004.02.005

[25]. S. Celik, DFT investigations and molecular docking as potent inhibitors of SARS-CoV-2 main protease of 4-phenylpyrimidine, Journal of Molecular Structure 1277 (2023) 134895. DOI: 10.1016/j.molstruc.2022.134895

[26]. V.H. Rezvan, Advanced Journal of Chemistry-Section A Molecular Structure, Molecular Structure, Optical Properties and Frontier Molecular Orbitals for Some of the 4-Substituted Cinnolines: Ab initio Calculations, Advanced Journal of Chemistry-Section A 5 (2022) 10-21. DOI: 10.22034/AJCA.2021.296241.1273

[27]. V.B. Sulimov, D.C. Kutov, A.V. Sulimov, Advances in docking, Current Medicinal Chemistry 26 (2019) 7555-7580. DOI: 10.2174/0929867325666180904115000

[28]. Z. Feng, N. Verdiguel, L. Chen, L.D. Costanzo, D.S. Goodsell, J.D. Westbrook, S.K. Burley, C. Zardecki, Impact of the protein data bank across scientific disciplines, Data Science Journal 19 (2020) 25 1-14. DOI: 10.5334/DSJ-2020-025

[29]. C.M.P. Rao, K. Silakabattini, N. Narapusetty, V.J.P. Marabathuni, K. Thejomoorthy, T.Y.S. Rajeswari, Insights from the molecular docking and simulation analysis of P38 MAPK phytochemical inhibitor complexes, Bioinformation 19 (2023) 323-330. DOI: 10.6026/97320630019323

[30]. Y. Gu, Z. Yu, Y. Wang, L. Chen, C. Lou, C. Yang, W. Li, G. Liu, Y. Tang, admetSAR3.0: a comprehensive platform for exploration, prediction and optimization of chemical ADMET properties, Nucleic Acids Research 52 (2024) 432-438. DOI: 10.1093/NAR/GKAE298

[31]. D.A. Filimonov, A. Lagunin, T. Gloriozova, A.V. Rudik, Prediction of the biological activity spectra of organic compounds using the pass online web resource, Biomedical Chemistry: Research and Methods 50 (2014) 444-457. DOI: /10.1007/S10593-014-1496-1/METRICS

[32]. R. Gandhimathi, S. Dheivamalar, R. Dhanasekaran, Geometry optimization, HOMO and LUMO energy, molecular electrostatic potential, NMR, FT-IR and FT-Raman analyzes on 4-nitrophenol, The European Physical Journal Applied Physics 69 (2015) 10202. DOI: 10.1051/EPJAP/2014140426

[33]. K.S. Kumar, N. Haridharan, S. Ranjith, A. Nataraj, Studies on the DFT calculations and molecular docking of versatile molecular sensor 1-(6-aminopyridin-2-yl) -3-(4-nitrophenyl) urea, Chemical Physics Impact 6 (2023) 100139. DOI: 10.1016/J.CHPHI.2022.100139

[34]. D.D.Y. Setsoafia, K.S. Ram, H. Mehdizadeh-Rad, D. Ompong, V. Murthy, J. Singh, DFT and TD-DFT calculations of orbital energies and photovoltaic properties of small molecule donor and acceptor materials used in organic solar cells, Journal of Renewable Materials 10 (2022) 2553-2567. DOI: 10.32604/JRM.2022.020967

[35]. S.M.A. Kawsar, H.A. Ara, S.A. Uddin, M.K. Hossain, S.A. Chowdhury, A.F.M. Sanaullah, M.A. Manchur, I. Hasan, Y. Ogawa, Y. Fujii, Y. Koide, Y. Ozeki, Chemically modified uridine molecules incorporating acyl residues to enhance antibacterial and cytotoxic activities, International Journal of Organic Chemistry 5 (2015) 232-245. DOI: 10.4236/IJOC.2015.54023

[36]. M.Z. Rana, M.R. Munshi, M.Al Masud, M.S. Zahan, Structural, electronic, optical and thermodynamic properties of $AlAuO_2$ and $AlAu_{094}Fe_{006}O_2$ compounds scrutinized by density

functional theory (DFT), Heliyon 9 (2023) 21405. DOI: 10.1016/j.heliyon.2023.e21405

[37]. R. Tabassum, S.M.A. Kawsar, A. Alam, S. Saha, A. Hosen, I. Hasan, Prinsa, M. Chalkha, Synthesis, spectral characterization, biological, FMO, MEP, molecular docking, and molecular dynamics simulation studies of cytidine derivatives as antimicrobial and anticancer agents, Chemical Physics Impact 9 (2024) 100724. DOI: 10.1016/j.chphi.2024.100724

[38]. S.L. Dhonnar, N.V. Sadgir, V.A. Adole, B.S. Jagdale, Molecular Structure, FT-IR Spectra, MEP and HOMO-LUMO investigation of 2-(4-fluorophenyl)-5-phenyl-1, 3,4-oxadiazole using DFT theory calculations, Advanced Journal of Chemistry Section A 4 (2021) 220-230. DOI: 10.22034/AJCA.2021.283003.1254

[39]. J.I. Aihara, Reduced HOMO−LUMO gap as an index of kinetic stability for polycyclic aromatic hydrocarbons, Journal of Physical Chemistry A 103 (1999) 7487-7495. DOI: 10.1021/JP990092I

[40]. D. Villemin, T. Abbaz, A. Bendjeddou, Molecular structure, HOMO, LUMO, MEP, natural bond orbital analysis of benzo and anthraquinodimethane derivatives, Pharmaceutical and Biological Evaluations 5 (2018) 27. DOI: 10.26510/2394-0859.PBE.2018.04

[41]. S.S. Pathade B.S. Jagdale, Synthesis and DFT-based quantum chemical studies of 2-(3-bromophenyl)-4-(4-bromophenyl)-2,3-dihydro-1H-1,5-benzodiazepine, Journal of Advanced Scientific Research 11 (2020) 87-94. https://www.sciensage.info/index.php/JASR/article/view/829

[42]. P. Geerlings, From Density Functional Theory to Conceptual Density Functional Theory and Biosystems, Pharmaceuticals 15 (2022) 1112. DOI: 10.3390/PH15091112

[43]. R.G. Pearson, Absolute electronegativity and hardness correlated with molecular orbital theory, Proceedings of the National Academy of Sciences 83 (1986) 8440-8441. DOI: 10.1073/PNAS.83.22.8440

[44]. H. Lafridi, F.A. Almalki, T. Ben Hadda, M. Berredjem, S.M.A. Kawsar, A.M. Alqahtani, E.R. Esharkawy, B. Lakhrissi, H. Zgou, *In silico* evaluation of molecular interactions between macrocyclic inhibitors with the HCV NS3 protease. Docking and identification of antiviral pharmacophore site, Journal of Biomolecular Structure and Dynamics 41 (2023) 2260-2273. DOI: 10.1080/07391102.2022.2029571

[45]. M. Sheikhi, E. Balali, H. Lari, Theoretical investigations on molecular structure, NBO, HOMO-LUMO and MEP analysis of two crystal structures of N-(2-benzoyl-phenyl) oxalyl: A DFT study, Journal of Physical & Theoretical Chemistry 13 (2016) 155-169.

[46]. A. Ramazani, M. Sheikhi, H. Ahankar, M. Rouhani, S.W. Jon, K. Slepokura, T. Lis, Crystal Structure, Spectroscopic and DFT Studies on E and Z Isomers of Ethyl 2-(2,3-dioxo-2,3-dihydro-1H-indol-1-yl)-3-phenyl-2-propenoate, Journal of Chemical Crystallography 47 (2017) 198-207. DOI: 10.1007/S10870-017-0697-8/METRICS

[47]. L. Li, C. Wu, Z. Wang, L. Zhao, Z. Li, C. Sun, T. Sun, Density functional theory (DFT) and natural bond orbital (NBO) study of vibrational spectra and intramolecular hydrogen bond interaction of l-ornithine–l-aspartate, Spectrochimica Acta Part A: Molecular and Biomolecular Spectroscopy 136 (2015) 338-346. DOI: 10.1016/J.SAA.2014.08.153

[48]. N. Issaoui, H. Ghalla, S. Muthu, H.T. Flakus, B. Oujia, Molecular structure, vibrational spectra, AIM, HOMO–LUMO, NBO, UV, first order hyperpolarizability, analysis of 3-thiophenecarboxylic acid monomer and dimer by Hartree–Fock and density functional theory, Spectrochimica Acta Part A: Molecular and Biomolecular Spectroscopy 136 (2015) 1227-1242. DOI: 10.1016/J.SAA.2014.10.008

[49]. P.C. Agu, C.A. Afiukwa, O.U. Orji, E.M. Ezeh, I.H. Ofoke, C.O. Ogbu, E.I. Ugwuja, P.M. Aja, Molecular docking as a tool for the discovery of molecular targets of nutraceuticals in diseases management, Scientific Reports 13 (2023) 1-18. DOI: 10.1038/S41598-023-40160-2;SUBJMETA

[50]. M. Chaudhary, K. Tyagi, A Review on Molecular Docking and its Application, International Journal of Advanced Research 12 (2024) 1141-1153. DOI: 10.21474/IJAR01/18505

[51]. N.S. Munia, M.A. Hosen, K.M.A. Azzam, M. Al-Ghorbani, M. Baashen, M.K. Hossain, F. Ali, S. Mahmud, M.S.S. Shimu, F.A. Almalki, T.B. Hadda, H. Laaroussi, S. Naimi, S.M.A. Kawsar, Synthesis, antimicrobial, SAR, PASS, molecular docking, molecular dynamics and pharmacokinetics studies of 5′-*O*-uridine derivatives bearing acyl moieties: POM study and identification of the pharmacophore sites, Nucleosides Nucleotides Nucleic Acids 41 (2022) 1036-1083. DOI: 10.1080/15257770.2022.2096898

[52]. H.M. Berman, J. Westbrook, Z. Feng, G. Gilliland, T.N. Bhat, H. Weissig, I.N. Shindyalov, P.E. Bourne, The Protein Data Bank, Nucleic Acids Research 28 (2000) 235-242. DOI: 10.1093/NAR/28.1.235

[53]. [S.M.A. Kawsar, F.A. Almalki, T.B. Hadd, H. Laaroussi, M.A.R. Khan, M.A. Hosen, S. Mahmud, A. Aounti, N.M.P. Maideen, F. Heidarizadeh, S.S.M. Soliman, Potential antifungal activity of novel carbohydrate derivatives validated by POM, molecular docking and molecular dynamic simulations analyses, Molecular Simulation 49 (2023) 60-75. DOI: 10.1080/08927022.2022.2123948

[54]. J. Perlstein, The Weak Hydrogen Bond in Structural Chemistry and Biology, Journal of the American Chemical Society 123 (2000) 191-192. DOI: 10.1021/JA0047368

[55]. J. Ferdous, F.A. Qais, F. Ali, D. Palit, I. Hasan, S.M.A. Kawsar, FTIR, ^{1}H-/^{13}C-NMR spectral characterization, antimicrobial, anticancer, antioxidant, anti-inflammatory, PASS, SAR, and

in silico properties of methyl α-D-glucopyranoside derivatives, Chemical Physics Impact 9 (2024) 100753. DOI: 10.1016/j.chphi.2024.100753

[56]. S.M.A. Kawsar, M.A. Hossain, S. Saha, E.M. Abdallah, A.R. Bhat, S. Ahmed, J. Jamalis, Y. Ozeki, Nucleoside-Based Drug Target with General Antimicrobial Screening and Specific Computational Studies against SARS-CoV-2 Main Protease, ChemistrySelect 9 (2024) 202304774. DOI: 10.1002/SLCT.202304774

[57]. S. Saha, V. Gupta, M.A. Hossain, Prinsa, J. Ferdous, K.B. Lokhande, V. Jakhmola, S.M.A. Kawsar, Computational Investigation of the Unveils NSD2 Inhibition Potential of *Berberis vulgaris*, *Sambucus nigra*, and *Morus alba* through Virtual Screening, Molecular Docking, MD Simulation, and DFT Analyses, Karbala International Journal of Modern Science 11 (2025), 129–143. DOI: 10.33640/2405-609X.3391

[58]. U. Norinder, C.A.S. Bergström, Prediction of ADMET Properties, ChemMedChem 1 (2006) 920-937. DOI: 10.1002/CMDC.200600155

[59]. D.A. Filimonov, D. Druzhilovskiy, A. Lagunin, T. Gloriozova, A. Rudik, A. Dmitriev, P. Pogodin, V. Poroikov, Computer-aided Prediction of Biological Activity Spectra for Chemical Compounds: Opportunities and Limitations, Biomedical Chemistry: Research and Methods 1 (2018) 4. DOI: 10.18097/BMCRM00004

[60]. D.S. Druzhilovskiy, A.V. Rudik, D.A. Filimonov, Computational platform Way2Drug: from the prediction of biological activity to drug repurposing, Russian Chemical Bulletin 66 (2017) 1832-1841. DOI: 10.1007/S11172-017-1954-X/METRICS

Received: 06.12.2025
Received in revised form: 24.12.2025
Accepted: 30.12.2025